

Response to referee comments

We thank the referee for their thorough review and helpful suggestions. The reviewer's comments (in black) and our responses follow.

General comments

This paper investigates – using the GEOS-Chem global chemical transport model - how surface deposition of divalent mercury species (Hg(II)) is influenced by Hg(II) production at different atmospheric heights. The authors show that surface deposition is dominated by production in the upper and middle troposphere and highlight the large role of subtropical anticyclones as a global reservoir of Hg(II). This study also shows that regional decreases in anthropogenic mercury emissions will not lead to a proportional regional decrease in wet deposition. The paper is organized clearly, easy to follow, well written, and will make a valuable contribution to the literature. However, I find the evaluation of the model with observations insufficient and not up to date. This paper will be suitable for publication after the authors address the following issues.

Following the reviewer's recommendation, we have significantly expanded our model-observation comparison to include sites outside the MDN, EMEP and AMNet networks.

Hg(II) concentrations: We have added comparisons with 14 sites measuring surface Hg(II) concentrations. These include stations from the worldwide GMOS network and stations in China, Taiwan, Germany, and Canada.

Hg wet deposition: We have added comparisons with 14 sites measuring Hg wet deposition. These include stations from the worldwide GMOS network and stations in China, Taiwan and Puerto Rico, US.

High-elevation sites: The 14 additional Hg(II) surface sites include 5 high-elevation sites (elevation > 1500m).

Aircraft-based observations: We have also added model-measurement comparison for 2 aircraft campaigns: the campaign over Tullahoma, TN and NOMADSS.

These comparisons are shown in Figs. S1, S2 and S3 that will be included in the supplement to the manuscript and are also displayed at the end of this document. A description of these measurements that will be included in the manuscript is below.

“Ground-based measurements of Hg wet deposition and Hg(II) surface concentration have been made as part of the Global Mercury Observations System (GMOS) network (Angot et al., 2014; Wängberg et al., 2016; Sprovieri et al., 2016, 2017; Travnikov et al., 2017), and at sites in Europe (Weigelt et al., 2013), Canada, and East Asia (Sheu et al., 2010; Sheu and Lin, 2013; Fu et al., 2015, 2016). We use the 2013-2014 measurements wherever available, but use all sites with one year or more of observations. We exclude sites in China classified as urban, because of proximity to large Hg(II) sources. We include 14 sites with annual-mean measurements of Hg wet deposition (Table S1), and 14 sites with annual-mean measurements of surface Hg(II) (Table S2).”

“We also include aircraft-based measurements of Hg(II) carried out near Tullahoma, Tennessee, USA from August 2012 to June 2013 (Brooks et al., 2014).”

Major comments: Comparison with observations

The two-year simulation (2012-2014) is evaluated with ground-based observations of Hg(II) concentrations and wet deposition. Section 2.2.3 concludes that the simulation reproduces quite well the spatial distribution and seasonal cycle of Hg(II) and wet deposition over the US but displays a 46% underestimate of wet deposition observed at EMEP sites. So what? How might this uncertainty affect the distribution of the tagged Hg(II) and ultimately their contributions to wet/dry distribution fluxes in different regions of the world?

It suggests that the production of Hg(II) in the free-troposphere over Europe is underestimated which would lead to an underestimate in the contribution of UT and MT tracers.

We have added the following paragraph to Sect. 3.2 in response to this and your other similar question below.

“In Sect. 2.2.3 we saw that the model overestimated observed wet deposition of Hg(II) over southeast U.S. during winter and spring. As a result, our estimate of the contribution of UT and MT tracers is likely an overestimate for this region and season. From our model evaluation, we had also concluded that our free-tropospheric Hg(II) production was too slow over Europe and, possibly, other regions north of 45°N. This suggests an underestimate of the concentrations of modeled UT and MT tracers in these regions.”

Additionally, the model is evaluated over the US and Europe only, using ground-based observations. The authors should consider using recent data from ground-based sites, aircraft campaigns and high-altitude sites to evaluate the model in different regions of the world and at different heights. To me, evaluating a model used to investigate the global distribution of Hg(II) at different heights a) over the US only, and b) at ground level only is not convincing enough. To address this concern, we have significantly expanded our model-observation comparison to include 14 additional stations measuring Hg wet deposition, 14 additional stations measuring Hg(II) surface concentrations, and 2 aircraft-based campaigns (the campaign over Tullahoma, TN and NOMADSS). Tables S1 and S2, and Figs. S1, S2 and S3 displayed at the end of the document will be included in the supplement to the manuscript.

1. Ground-based observations

1.1 Hg(II) concentrations The authors use the 2009-2012 AMNet observations to evaluate the model over the US. I understand that the authors use data that are publicly available. However, evaluating 2013-2014 model outputs with 2009-2012 observations is not satisfying unless inter-annual variability is discussed at some point.

Good point. From the 4-year (2013-16) “dry-Hg(II)” simulation, we find that the variation in the modeled 2-year average Hg(II) concentrations at the AMNet sites vary by $\pm 30\%$.

We have added the following to Sect 2.3.3 “Comparing observations and simulations for different time periods adds additional uncertainty due to inter-annual variations. From four years of model simulation (2013-16), we estimate this uncertainty at $\pm 30\%$.”

In Europe, the authors highlight a discrepancy between modeled/observed wet deposition and suggest that this could “indicate an underestimate in the modeled Hg(II) concentrations over the region”. The authors could easily check that since Hg(II) data are available for 2013-2014 (Sprovieri et al., 2016) at Iskrba (Slovenia), Longobucco (Italy), and Rao (Sweden – see also Wängberg et al., 2016). Additionally, how well can the model reproduce Hg(II) concentrations elsewhere? Still according to Sprovieri et al. (2016), Hg(II) data are available around the world for years 2013-2014 at Amsterdam Island (see also Angot et al., 2014), Bariloche (Argentina), Cape Hedo (Japan), Manaus (Brazil), and Minamata (Japan).

We have expanded our model-observation comparison to include 14 additional stations measuring Hg(II) surface concentration, which include GMOS sites for which Hg(II) observations have been published. See Tables S2 and Fig. S2. These comparisons show a reasonable model performance (NMB:-9%, FAC2:50%). Modeled surface Hg(II) concentrations at Rão and Longobucco are in good agreement with the observations (Fig. S2). However, it should be noted that an underestimate in Hg wet deposition reflects an underestimate in the abundance of Hg(II) in the precipitating column which is 1-5 km high typically, and may not be detected from the surface Hg(II) measurements. Comparison with wet deposition measurements at Iskrba and Mace Head also show a model underestimate of 25% in Hg concentration in wet deposition.

1.2 Wet deposition Same as above, why don't the authors use recent wet deposition data collected around the world to evaluate the model in different regions of the world? A recent paper (Sprovieri et al., 2017) present seasonal and annual variations of Hg wet deposition and concentration collected at 17 ground-based sites in the Northern and Southern Hemispheres as part of the GMOS project.

We have significantly expanded our model-observation comparison to include 14 additional stations measuring Hg wet deposition, which include GMOS sites for which Hg wet deposition measurements have been published in Sprovieri et al. (2017). See Tables S1 and Fig. S1. The model reproduces the wet deposition observations with a NMB of 52% and FAC2 of 64%, and the VWM concentrations with a NMB of 48% and FAC2 of 78%.

Additionally, page 9, lines 2-4: "Over the southeast US, the modeled VWM concentrations are higher than observations during winter and spring, suggesting a model overestimate in atmospheric Hg(II) concentrations in that region or an overestimate in the amount of Hg(II) scavenged by precipitation". If the model overestimates the amount of Hg(II) scavenged by precipitation, what is the possible influence on results presented in section 3.2, i.e. on the modeled contribution of MT and UT? I would like to see a discussion on how results presented in section 2.2.3 (comparison of modeled and measured Hg(II)) affect results presented thereafter. See our response to a similar question above.

2. Vertical profiles

The authors should consider using recent data from aircraft campaigns and high- elevation sites to evaluate the model in different regions of the world. How well can the model reproduce these observations (see for instance Bieser et al., 2016).

2.1 Aircraft campaigns An evaluation of the model is done, over the US, in a previous paper (Shah et al., 2016) during the NOMADSS campaign. The authors could refer to this paper here. Within the GMOS project, vertical profiles were taken on board research aircraft in August 2013 in background air over different locations in Slovenia and Germany (Weigelt et al., 2016). Additionally, Hg(0), Hg(II), and Hg(p) profiles were collected on 28 flights between August 2012 and July 2013 (1000 to 6000 m, Brooks et al., 2014). Finally, the authors could use data from the intercontinental flights between Germany and North/South America under the umbrella of the CARABIC project (Slemr et al., 2014, 2016).

We have expanded our model-observation comparison to include two aircraft-based campaigns (NOMADSS and the one of over Tullahoma, TN). The model captures the Hg(II) vertical profiles observed during these two aircraft campaigns. See Fig. S3. For observations over Tullahoma, TN we find the model NMB of 14% and FAC2 of 52%. For observations above 4 km in the NOMADSS campaign, the model NMB is -29% and FAC2 is 53%.

2.2 High-elevation ground sites The authors could use data collected at various high- elevation sites such as Mt. Walinguan (China), Mt. Ailao (China), Kodaicanal (India), Everest/K2 (Nepal) and Col Margherita (Italy) (Sprovieri et al., 2016) to evaluate Hg(0) and/or Hg(II) concentrations. Note that mercury data discussed in this paper are available upon request at: <http://sdi.iia.cnr.it/geoint/publicpage/GMOS/gmos.historical.zul>.

Five of the 14 additional Hg(II) sites are at high-elevations. See Table S2 and Fig. S2. We find that in general the model captures the relatively higher concentrations observed at these high-elevation sites.

Other comments: Model sensitivity to oxidation chemistry and emission speciation

The authors perform an additional one-year sensitivity simulation using the original GEOS-Chem Br concentrations instead of the 3 times Br concentrations in the base simulation. Given that

updates by Schmidt et al. (2016) have resulted in an improved agreement with satellite and in situ observation of BrO, I wonder why the authors did not perform an additional simulation using these updated fields. Page 9, line 17: “suggesting that the modeled oxidation rate is too slow over this region”. Using Br fields from Schmidt et al. (2016), i.e., a factor 2.3 increase in free tropospheric Br concentrations north of 45N might lead to a better agreement between modeled/observed data over Europe.

The bromine fields from Schmidt et al. (2016) have just recently been incorporated into the GEOS-Chem Hg simulation (Horowitz et al., 2017). Therefore, we weren't able to use those fields in our simulations.

Page 12, lines 24-33. How do these results compare to the results by Bieser et al. (2016)? According to the latter, “high RM concentrations in the UT could be reproduced by oxidation by Br while elevated concentrations in the LT were better reproduced by OH and ozone”. Does it sound feasible and adequate to implement two different mechanisms in GEOS-Chem depending on the altitude?

Bieser et al. (2017) did not investigate the vertical profile with the OH/O₃ oxidation mechanism in GEOS-Chem. They also show that the inter-model variation in the simulated Hg(II) concentrations is larger than the observed variation in the Hg(II) vertical profiles, thus not providing much support for considering an altitude-dependent mechanism in GEOS-Chem. The results of our simulation, using Br chemistry, show good agreement with the aircraft-based observations over Tullahoma, TN (Fig. S3 panel a) and with surface observations at AMNet sites (Fig. 3)

Line by line comments

Section 2.2: Which version of GEOS-Chem do you use?

It is v9-02. We have added the following sentence to the manuscript in Sect. 2.2: “We use GEOS-Chem v9-02 (<http://acmg.seas.harvard.edu/geos/>).”

Page 8, lines 18-20: “The model reproduces the observed seasonal variations in the central and northeast regions, but underestimates the summer deposition fluxes in the southeast because of a factor of 2 underestimate in summertime precipitation by the GEOS-FP meteorological fields”. Is that also the case for other (GEOS-5, MERRA) meteorological fields? If not, why don't the authors use them? MERRA meteorological data are available for 2013-2014.

The MERRA precipitation over the SE US during summer is closer to observations. Although it is not possible for us to redo the model setup and simulations with a new meteorological field for this study, it is something we can investigate fully in the GEOS-Chem Hg simulation in the future.

Page 9, line 2: there is a typo “Over the southeast US, tmodeled (. . .)”.
Fixed the typo.

Page 9, lines 10-12: “(. . .) likely because the upward scaling of the Br concentrations in our simulation did not extend north of 45N and covered only parts of Southern Europe”. Could you please add the latitude on the various figures?

We have added latitude and longitude grids to maps in Figures 1, 2, 3, 5, and 7.

Figure 4e: I am just curious; how can you explain the elevated contribution of MT tracer over the Antarctic continent?

The high elevation of the Antarctic (~2500 m) means that much of the surface is higher than the upper boundary of the lower troposphere (defined here as region below 750 hPa), thus we see elevated contribution from the MT tracer.

Figure 10b: Why is NY95 excluded from the regression calculation? I agree that it is an outlier here, but the question is why? According to info found on AMNet website (and not in the paper. . .), the collection of Hg(II) concentrations stopped in November 2009 at this site. This suggests that the authors only have a few months of data at this site, and not data for the entire 2009-2012 period. That kind of information would be useful (in supplementary?) in order to get a better insight on which observation data are used to evaluate the model.

We agree, and have added two tables in the supplement (Tables S1 and S2, also included at the end of the document) with the details of sites, including their measurement time periods, used in the paper.

The NY95 site was operational from 2009 to 2012. We can't tell why it is an outlier. It is possible that we are missing a Hg(II) emission source close to the site. However, we would like to refer to Gay et al. (2013), page 11345, for a discussion on the GOM and PBM variations at the AMNet sites.

Table S1: List of stations with observations of Hg wet deposition used in this study

Site ID	Site Name	Latitude	Longitude	Elevation (m.a.s.l.)	Measurement period	Network/Region
CO96	Molas Pass	37.75	-107.69	3248	2013-2014	MDN ^a
FL11	Everglades National Park-Research Center	25.39	-80.68	2	2013-2014	MDN
WA18	Seattle/NOAA	47.68	-122.26	11	2013-2014	MDN
TX21	Longview	32.38	-94.71	103	2013-2014	MDN
VT99	Underhill	44.53	-72.87	399	2013-2014	MDN
VA28	Shenandoah National Park-Big Meadows	38.52	-78.43	1072	2013-2014	MDN
WI36	Trout Lake	46.05	-89.65	509	2013-2014	MDN
WI99	Lake Geneva	42.58	-88.50	288	2013-2014	MDN
PA29	Kane Experimental Forest	41.60	-78.77	618	2013-2014	MDN
PA42	Leading Ridge	40.66	-77.94	287	2013-2014	MDN
PA72	Milford	41.33	-74.82	212	2013-2014	MDN
TN11	Great Smoky Mountains	35.66	-83.59	640	2013-2014	MDN
MN18	Fernberg	47.95	-91.50	524	2013-2014	MDN
ME02	Bridgton	44.11	-70.73	222	2013-2014	MDN
ME96	Casco Bay-Wolfe's Neck Farm	43.83	-70.06	15	2013-2014	MDN
NC08	Waccamaw State Park	34.26	-78.48	10	2013-2014	MDN
PA13	Allegheny Portage Historic Site	40.46	-78.56	739	2013-2014	MDN
PA90	Hills Creek State Park	41.80	-77.19	476	2013-2014	MDN
SC19	Congaree Swamp	33.81	-80.78	34	2013-2014	MDN
IL11	Bondville	40.05	-88.37	212	2013-2014	MDN
FL34	Everglades Nutrient Removal Project	26.66	-80.40	10	2013-2014	MDN
FL05	Chassahowitzka National Wildlife Refuge	28.75	-82.56	3	2013-2014	MDN
GA09	Okefenokee National Wildlife Refuge	30.74	-82.13	45	2013-2014	MDN
PA00	Arendtsville	39.92	-77.31	269	2013-2014	MDN
KS32	Lake Scott State Park	38.67	-100.92	863	2013-2014	MDN
ME98	Acadia National Park-McFarland Hill	44.38	-68.26	150	2013-2014	MDN
ME00	Caribou	46.87	-68.01	191	2013-2014	MDN
ME09	Greenville Station	45.49	-69.66	322	2013-2014	MDN
MN16	Marcell Experimental Forest	47.53	-93.47	431	2013-2014	MDN
MN23	Camp Ripley	46.25	-94.50	410	2013-2014	MDN
MN27	Lamberton	44.24	-95.30	367	2013-2014	MDN
MO03	Ashland Wildlife Area	38.75	-92.20	257	2013-2014	MDN
MT05	Glacier National Park-Fire Weather Station	48.51	-114.00	964	2013-2014	MDN
NE15	Mead	41.15	-96.49	352	2013-2014	MDN
NY20	Huntington Wildlife	43.97	-74.22	500	2013-2014	MDN
NY68	Biscuit Brook	41.99	-74.50	634	2013-2014	MDN
PA37	Waynesburg	39.82	-80.29	452	2013-2014	MDN
MI48	Seney National Wildlife Refuge-Headquarters	46.29	-85.95	220	2013-2014	MDN
SC05	Cape Romain National Wildlife Refuge	32.94	-79.66	1	2013-2014	MDN
SC03	Savannah River	33.25	-81.65	90	2013-2014	MDN
PA60	Valley Forge	40.12	-75.88	46	2013-2014	MDN
PA30	Erie	42.16	-80.11	177	2013-2014	MDN

Table S1 continued

Site ID	Site Name	Latitude	Longitude	Elevation	Measurement	Network/
AL03	Centreville	32.90	-87.25	135	2013-2014	MDN
GA40	Yorkville	33.93	-85.05	395	2013-2014	MDN
MO46	Mingo National Wildlife Refuge	36.97	-90.14	105	2013-2014	MDN
KY10	Mammoth Cave National Park	37.13	-86.15	236	2013-2014	MDN
MS22	Oak Grove	30.98	-88.93	100	2013-2014	MDN
WI31	Devil's Lake	43.44	-89.68	389	2013-2014	MDN
PA47	Millersville	39.99	-76.39	84	2013-2014	MDN
GA33	Sapelo Island	31.40	-81.28	3	2013-2014	MDN
OK99	Stilwell	35.75	-94.67	299	2013-2014	MDN
NV02	Lesperance Ranch	41.50	-117.50	1388	2013-2014	MDN
MD99	Beltsville	39.03	-76.82	46	2013-2014	MDN
MD08	Piney Reservoir	39.71	-79.01	769	2013-2014	MDN
NJ30	New Brunswick	40.47	-74.42	21	2013-2014	MDN
ON07	Egbert	44.23	-79.79	196	2013-2014	MDN
WI10	Potawatomi	45.56	-88.81	570	2013-2014	MDN
WA03	Makah National Fish Hatchery	48.29	-124.65	6	2013-2014	MDN
CA94	Converse Flats	34.19	-116.91	1724	2013-2014	MDN
CA20	Yurok Tribe-Requa	41.56	-124.09	110	2013-2014	MDN
OK01	McGee Creek	34.32	-95.89	195	2013-2014	MDN
OK31	Copan	36.91	-95.88	255	2013-2014	MDN
SD18	Eagle Butte	44.99	-101.24	742	2013-2014	MDN
MD00	Smithsonian Environmental Research Center	38.89	-76.56	20	2013-2014	MDN
FL97	Everglades-Western Broward County	26.17	-80.82	4	2013-2014	MDN
UT97	Salt Lake City	40.71	-111.96	1297	2013-2014	MDN
OK04	Lake Murray	34.10	-97.07	245	2013-2014	MDN
PA52	Little Pine State Park	41.36	-77.36	228	2013-2014	MDN
KS03	Reserve	39.98	-95.57	265	2013-2014	MDN
KS24	Glen Elder State Park	39.51	-98.34	456	2013-2014	MDN
KS99	Cimarron National Grassland	37.13	-101.82	1021	2013-2014	MDN
OK06	Wichita Mountains	34.73	-98.71	492	2013-2014	MDN
KS04	West Mineral	37.27	-94.94	274	2013-2014	MDN
NY43	Rochester	43.15	-77.55	136	2013-2014	MDN
NY06	Bronx	40.87	-73.88	68	2013-2014	MDN
MN98	Blaine	45.14	-93.22	275	2013-2014	MDN
MS12	Grand Bay NERR	30.43	-88.43	2	2013-2014	MDN
PA21	Goddard State Park	41.43	-80.15	385	2013-2014	MDN
FL96	Pensacola	30.55	-87.38	45	2013-2014	MDN
AL19	Birmingham	33.55	-86.81	200	2013-2014	MDN
DE0008R	Schmücke	50.65	10.77	937	2013-2014	EMEP ^b
FI0036R	Pallas (Matorova)	68.00	24.24	340	2013-2014	EMEP
GB0036R	Harwell	51.57	-1.32	137	2013-2014	EMEP
GB0048R	Auchencorth Moss	55.79	-3.24	260	2013-2014	EMEP
NO0001R	Birkenes	58.38	8.25	190	2013-2014	EMEP
SE0005R	Bredkålen	63.85	15.33	404	2013-2014	EMEP
SE0011R	Vavihill	56.02	13.15	175	2013-2014	EMEP
SE0014R	Råö	57.39	11.91	5	2013-2014	EMEP
NYA	Ny-Ålesund	78.90	11.88	12	2013-2014	GMOS ^c
MHE	Mace Head	53.33	-9.91	5	2013	GMOS
ISK	Iskrba	45.56	14.86	520	2013-2014	GMOS
SIS	Sisal	21.16	-90.05	7	2013-2014	GMOS
AMS	Amsterdam Island	-37.80	77.55	3	2013-2014	GMOS

Table S1 continued

Site ID	Site Name	Latitude	Longitude	Elevation	Measurement	Network/
CGR	Cape Grim	-40.68	144.69	94	2013-2014	GMOS
MCB	Mt. Changbai	42.41	128.11	736	2011-2014	China ^d
MDM	Mt. Damei	29.63	121.57	550	2012-2014	China
MLG	Mt. Leigong	26.39	108.20	2176	2008-2009	China
MAL	Mt. Ailao	24.53	101.11	2450	2011-2014	China
MWA	Mt. Waliguan	36.29	100.90	3816	2012-2014	China
BYB	Bayinbuluk	42.89	83.72	2500	2013-2014	China
PEN	Pengjiayu	25.63	122.07	102	2009	Taiwan ^e
PR20	El Verde	18.32	-65.82	380	2015	MDN

(a) <http://nadp.sws.uiuc.edu/mdn/>

(b) <http://www.nilu.no/projects/ccc/index.html>

(c) Sprovieri et al. (2017)

(d) Fu et al. (2016)

(e) Sheu and Lin (2013)

Table S2: List of ground stations with observations of Hg(II) surface concentrations used in this study

Site ID	Site Name	Latitude	Longitude	Elevation (m.a.s.l.)	Measurement period	Network/Region
AL19	Birmingham	33.55	-86.81	177	2009-2012	AMNet ^a
CA48	Elkhorn Slough	36.81	-121.78	10	2010-2011	AMNet
FL96	Pensacola	30.55	-87.38	44	2009-2012	AMNet
GA40	Yorkville	33.93	-85.05	394	2009-2012	AMNet
MD08	Piney Reservoir	39.71	-79.01	761	2009-2012	AMNet
MD96	Beltsville_B	39.03	-76.82	47	2009-2012	AMNet
MD97	Beltsville	39.03	-76.82	47	2009-2012	AMNet
MS12	Grand Bay NERR	30.41	-88.40	1	2009-2012	AMNet
MS99	Grand Bay NERR_B	30.41	-88.40	1	2009-2012	AMNet
NH06	Thompson Farm	43.11	-70.95	25	2009-2011	AMNet
NJ05	Brigantine	39.46	-74.45	8	2009-2012	AMNet
NS01	Kejimikujik	44.43	-65.20	158	2009-2012	AMNet
NY06	New York City	40.87	-73.88	26	2009-2012	AMNet
NY20	Huntington Wildlife Forest	43.97	-74.22	502	2009-2012	AMNet
NY43	Rochester	43.15	-77.62	154	2009	AMNet
NY95	Rochester_B	43.15	-77.55	154	2009-2012	AMNet
OH02	Athens	39.31	-82.12	274	2009-2012	AMNet
OK99	Stilwell	35.75	-94.67	300	2009-2012	AMNet
PA13	Allegheny Portage	40.46	-78.56	739	2009-2012	AMNet
UT96	Antelope Island	41.09	-112.12	1285	2009-2011	AMNet
UT97	Salt Lake City	40.71	-111.96	1099	2009-2012	AMNet
VT99	Underhill	44.53	-72.87	397	2009-2012	AMNet
WI07	Horicon	43.46	-88.62	272	2009-2012	AMNet
WV99	Canaan Valley Institute	39.12	-79.45	985	2009-2012	AMNet
AMS	Amsterdam Island	-37.80	77.55	70	2012-13	GMOS ^b
RAO	Råö	57.39	11.91	7	2012-15	GMOS ^c
LON	Longobucco	39.39	16.61	1379	2013	GMOS ^d
MAN	Manaus	-2.89	-59.97	110	2013	GMOS ^d
WAL	Waldhof	52.80	10.76	74	2009-2011	Germany ^e
MCH	Mt. Changbai	42.40	128.11	740	2013-2014	China ^f
MWA	Mt. Waliguan	36.29	100.90	3816	2007-2008	China
MAL	Mt. Ailao	24.53	101.02	2450	2011-2012	China
SLA	Shangri-La	28.02	99.73	3580	2009-2010	China
MYU	Miyun	40.48	116.76	220	2008-2009	China
MDA	Mt. Damei	29.63	121.57	550	2011-2013	China
MGO	Mt. Gongga	29.65	102.12	1640	2005-2007	China
LABS	Lulin Atmospheric Background Station	23.51	120.92	2862	2006-2007	Taiwan ^g
ALE	Alert	82.49	-62.34	210	2009-2011	Canada ^h

(a) <http://nadp.sws.uiuc.edu/amn/>

(b) Angot et al. (2014)

(c) Wängberg et al. (2016)

(d) Travnikov et al. (2017)

(e) Weigelt et al. (2013)

(f) Fu et al. (2015)

(g) Sheu et al. (2010)

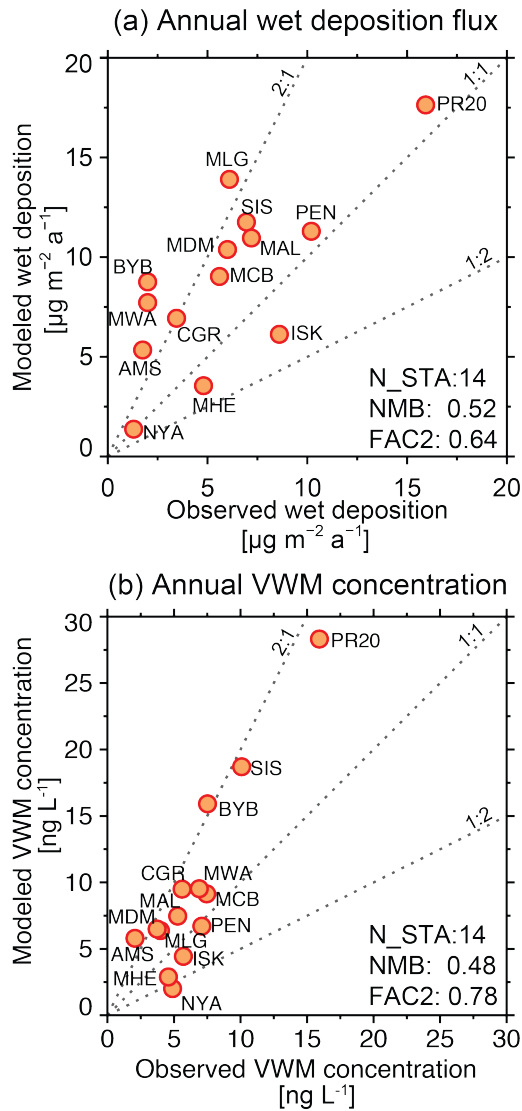


Figure S1 (a) Simulated and observed Hg wet deposition flux for GMOS and other stations listed in Table S1. (b) Simulated and observed annual volume-weighted mean (VWM) Hg concentration for GMOS and other stations listed in Table S1. The number of stations (N_STA), normalized mean bias (NMB; $\text{NMB} = \sum_i (M_i - O_i) / \sum_i O_i \times 100\%$), and FAC2 (percentage of points where $0.5 \leq M_i / O_i \leq 2$ where O_i and M_i are observed and simulated values, respectively) is included in both panels.

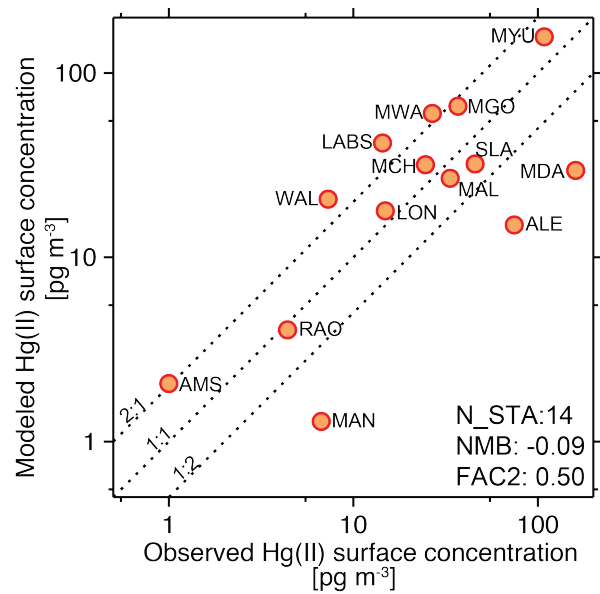


Figure S2 Simulated and observed surface Hg(II) concentration for GMOS and other stations listed in Table S1. Note the logarithmic scale on both axes.

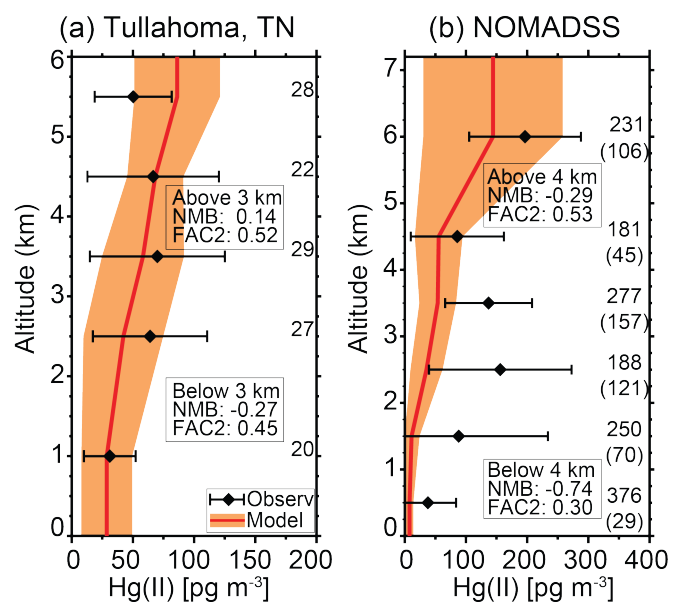


Figure S3 (a) Simulated and observed Hg(II) concentrations for aircraft-based campaign over Tullahoma, TN, USA (2012-2013) (Brooks et al., 2013). (b) Simulated and observed Hg(II) concentrations for the NOMADSS aircraft-based campaign (2013) (Shah et al., 2016). The number of model-observation pairs in each height bin is shown in panel (a). In panel (b), the number of model-observation pairs in each height bin, and, in parentheses, the number of model-observation pairs where the observations were above the instrument detection limit, are shown.

References

- Angot, H., Barret, M., Magand, O., Ramonet, M. and Dommergue, A.: A 2-year record of atmospheric mercury species at a background Southern Hemisphere station on Amsterdam Island, *Atmospheric Chem. Phys.*, 14(20), 11461–11473, doi:10.5194/acp-14-11461-2014, 2014.
- Bieser, J., Slemr, F., Ambrose, J., Brenninkmeijer, C., Brooks, S., Dastoor, A., DeSimone, F., Ebinghaus, R., Gencarelli, C. N., Geyer, B., Gratz, L. E., Hedgecock, I. M., Jaffe, D., Kelley, P., Lin, C.-J., Jaegle, L., Matthias, V., Ryjkov, A., Selin, N. E., Song, S., Travnikov, O., Weigelt, A., Luke, W., Ren, X., Zahn, A., Yang, X., Zhu, Y. and Pirrone, N.: Multi-model study of mercury dispersion in the atmosphere: vertical and interhemispheric distribution of mercury species, *Atmospheric Chem. Phys.*, 17(11), 6925–6955, doi:10.5194/acp-17-6925-2017, 2017.
- Brooks, S., Ren, X., Cohen, M., Luke, W. T., Kelley, P., Artz, R., Hynes, A., Landing, W. and Martos, B.: Airborne Vertical Profiling of Mercury Speciation near Tullahoma, TN, USA, *Atmosphere*, 5(3), 557, doi:10.3390/atmos5030557, 2014.
- Fu, X., Yang, X., Lang, X., Zhou, J., Zhang, H., Yu, B., Yan, H., Lin, C.-J. and Feng, X.: Atmospheric wet and litterfall mercury deposition at urban and rural sites in China, *Atmospheric Chem. Phys.*, 16(18), 11547–11562, doi:10.5194/acp-16-11547-2016, 2016.
- Fu, X. W., Zhang, H., Yu, B., Wang, X., Lin, C.-J. and Feng, X. B.: Observations of atmospheric mercury in China: a critical review, *Atmospheric Chem. Phys.*, 15(16), 9455–9476, doi:10.5194/acp-15-9455-2015, 2015.
- Gay, D. A., Schmeltz, D., Prestbo, E., Olson, M., Sharac, T. and Tordon, R.: The Atmospheric Mercury Network: measurement and initial examination of an ongoing atmospheric mercury record across North America, *Atmospheric Chem. Phys.*, 13(22), 11339–11349, doi:10.5194/acp-13-11339-2013, 2013.
- Horowitz, H. M., Jacob, D. J., Zhang, Y., Dibble, T. S., Slemr, F., Amos, H. M., Schmidt, J. A., Corbitt, E. S., Marais, E. A. and Sunderland, E. M.: A new mechanism for atmospheric mercury redox chemistry: implications for the global mercury budget, *Atmospheric Chem. Phys.*, 17(10), 6353–6371, doi:10.5194/acp-17-6353-2017, 2017.
- Schmidt, J. A., Jacob, D. J., Horowitz, H. M., Hu, L., Sherwen, T., Evans, M. J., Liang, Q., Suleiman, R. M., Oram, D. E., Le Breton, M., Percival, C. J., Wang, S., Dix, B. and Volkamer, R.: Modeling the observed tropospheric BrO background: Importance of multiphase chemistry and implications for ozone, OH, and mercury, *J. Geophys. Res. Atmospheres*, 121(19), 11,819–11,835, doi:10.1002/2015JD024229, 2016.
- Sheu, G.-R. and Lin, N.-H.: Characterizations of wet mercury deposition to a remote islet (Pengjiayu) in the subtropical Northwest Pacific Ocean, *Atmos. Environ.*, 77, 474–481, doi:10.1016/j.atmosenv.2013.05.038, 2013.
- Sheu, G.-R., Lin, N.-H., Wang, J.-L., Lee, C.-T., Yang, C.-F. O. and Wang, S.-H.: Temporal distribution and potential sources of atmospheric mercury measured at a high-elevation background station in Taiwan, *Atmos. Environ.*, 44(20), 2393–2400, doi:10.1016/j.atmosenv.2010.04.009, 2010.
- Slemr, F., Weigelt, A., Ebinghaus, R., Brenninkmeijer, C., Baker, A., Schuck, T., Rauthe-Schöch, A., Riede, H., Leedham, E., Hermann, M., van Velthoven, P., Oram, D., O'Sullivan, D., Dyroff, C., Zahn, A., Ziereis, H., 2014. Mercury Plumes in the Global Upper Troposphere Observed during Flights with the CARIBIC Observatory from May 2005 until June 2013. *Atmosphere* 5, 342–369. doi:10.3390/atmos5020342
- Slemr, F., Weigelt, A., Ebinghaus, R., Kock, H.H., Bödewadt, J., Brenninkmeijer, C.A.M., Rauthe-Schöch, A., Weber, S., Hermann, M., Becker, J., Zahn, A., Martins-son, B., 2016. Atmospheric mercury measurements onboard the CARIBIC passenger aircraft. *Atmos Meas Tech* 9, 2291–2302. doi:10.5194/amt-9-2291-2016

Sprovieri, F., Pirrone, N., Bencardino, M., D'Amore, F., Carbone, F., Cinnirella, S., Mannarino, V., Landis, M., Ebinghaus, R., Weigelt, A., Brunke, E.-G., Labuschagne, C., Martin, L., Munthe, J., Wängberg, I., Artaxo, P., Morais, F., Barbosa, H. D. M. J., Brito, J., Cairns, W., Barbante, C., Diéguez, M. D. C., Garcia, P. E., Dommergue, A., Angot, H., Magand, O., Skov, H., Horvat, M., Kotnik, J., Read, K. A., Neves, L. M., Gawlik, B. M., Sena, F., Mashyanov, N., Obolkin, V., Wip, D., Feng, X. B., Zhang, H., Fu, X., Ramachandran, R., Cossa, D., Knoery, J., Maruszczak, N., Nerentorp, M. and Norstrom, C.: Atmospheric mercury concentrations observed at ground-based monitoring sites globally distributed in the framework of the GMOS network, *Atmospheric Chem. Phys.*, 16(18), 11915–11935, doi:10.5194/acp-16-11915-2016, 2016.

Sprovieri, F., Pirrone, N., Bencardino, M., D'Amore, F., Angot, H., Barbante, C., Brunke, E.-G., Arcega-Cabrera, F., Cairns, W., Comero, S., Diéguez, M. D. C., Dommergue, A., Ebinghaus, R., Feng, X. B., Fu, X., Garcia, P. E., Gawlik, B. M., Hageström, U., Hansson, K., Horvat, M., Kotnik, J., Labuschagne, C., Magand, O., Martin, L., Mashyanov, N., Mkololo, T., Munthe, J., Obolkin, V., Ramirez Islas, M., Sena, F., Somersset, V., Spandow, P., Vardè, M., Walters, C., Wängberg, I., Weigelt, A., Yang, X. and Zhang, H.: Five-year records of mercury wet deposition flux at GMOS sites in the Northern and Southern hemispheres, *Atmospheric Chem. Phys.*, 17(4), 2689–2708, doi:10.5194/acp-17-2689-2017, 2017.

Travnikov, O., Angot, H., Artaxo, P., Bencardino, M., Bieser, J., D'Amore, F., Dastoor, A., De Simone, F., Diéguez, M. D. C., Dommergue, A., Ebinghaus, R., Feng, X. B., Gencarelli, C. N., Hedgecock, I. M., Magand, O., Martin, L., Matthias, V., Mashyanov, N., Pirrone, N., Ramachandran, R., Read, K. A., Ryjkov, A., Selin, N. E., Sena, F., Song, S., Sprovieri, F., Wip, D., Wängberg, I. and Yang, X.: Multi-model study of mercury dispersion in the atmosphere: atmospheric processes and model evaluation, *Atmospheric Chem. Phys.*, 17(8), 5271–5295, doi:10.5194/acp-17-5271-2017, 2017.

Wängberg, I., Nerentorp Mastromonaco, M. G., Munthe, J. and Gårdfeldt, K.: Airborne mercury species at the Råö background monitoring site in Sweden: distribution of mercury as an effect of long-range transport, *Atmospheric Chem. Phys.*, 16(21), 13379–13387, doi:10.5194/acp-16-13379-2016, 2016.

Weigelt, A., Temme, C., Bieber, E., Schwerin, A., Schuetze, M., Ebinghaus, R. and Kock, H. H.: Measurements of atmospheric mercury species at a German rural background site from 2009 to 2011 – methods and results, *Environ. Chem.*, 10(2), 102–110, doi:10.1071/EN12107, 2013.